 ICCES, vol.3, no.4, pp.177-188, 2007

A comparison of the RBF-based meshfree boundary knot and the boundary particle methods

W. Chen[1]

Summary

This paper is concerned with the two new boundary-type radial basis function collocation schemes, boundary knot method (BKM) and boundary particle method (BPM). The BKM is developed based on the dual reciprocity theorem, while the BKM employs the multiple reciprocity technique. Unlike the method of fundamental solution, the two methods use the non-singular general solution instead of the singular fundamental solution to circumvent the controversial artificial boundary outside the physical domain. Compared with the boundary element method, both BKM and BPM are meshfree, super-convergent, integration-free, symmetric, and mathematically simple collocation techniques for general PDEs. In particular, the BPM does not require any inner nodes for inhomogeneous problems. In this study, the accuracy, efficiency, and applicability of the two methods are numerically tested to some 2D, 3D Helmholtz, diffusion, and convection-diffusion problems under complicated geometries. Their advantages and disadvantages are compared and discussed based on numerical observations.

keywords: boundary knot method; boundary particle method; radial basis function; meshfree.

Introduction

In last decade much effort has been devoted to developing a variety of meshfree schemes for numerical partial differential equation (PDE) discretization. The driving force behind the scene is that the mesh-based methods such as the standard FEM and BEM often require prohibitively computational effort to mesh or remesh in handling high-dimensional, moving boundary, and complex-shaped boundary problems. Most meshfree techniques available today are based on using moving least square (MLS) strategy. In their weak-form fashion, a shadow element is still necessary for numerical integration rather than for function interpolation. Therefore, these methods are not truly meshfree.

The methods based on the radial basis function (RBF) are inherently meshfree due to the fact that the RBF method uses the one-dimensional distance variable irrespective of dimensionality of problems. Therefore, the RBF methods are independent of dimensionality and complexity of problem geometry. Nardini and Brebbia[1] in 1982 have actually applied the RBF concept to develop currently popular dual reciprocity BEM (DR-BEM) without a notion of "RBF". Only after Kansa's pioneer work [2] in 1990, the research on the RBF-based numerical

[1]Institute of Soft Matter Mechanics, Department of Engineering Mechanics, Hohai University, No. 1 Xikang Road, Nanjing City, Jiangsu Province 210098, China

schemes for PDEs has become very active. The RBF-based meshfree techniques in the collocation fashion are all truly meshfree without the need of any mesh at all.

Among the existing RBF schemes, the so-called Kansa's method is a domain-type collocation technique, while the method of fundamental solution (MFS), also known as the regular BEM versus singular BEM, is a classical boundary-type RBF collocation methodology. The MFS outperforms the standard BEM in its merits being integration free, convergence speed, easy-to-use, and meshfree.[3] On the other hand, the main drawback of the MFS is due to the use of the fictitious boundary outside the physical domain. The arbitrariness in the determination of the artificial boundary introduces such troublesome issues as instability in dealing with problems having complicated geometry and impedes the efficacy of the MFS to practical engineering problems.

Instead of using the singular fundamental solution, Chen and Tanaka[4] exploited the non-singular general solution to the approximation of the homogeneous solution and removed the controversial artificial boundary in the MFS. Like the MFS and DRBEM, the new method also employs the dual reciprocity method to approximate the particular solution. This method is called the boundary knot method (BKM). Some preliminary numerical experiments[4,5] show that the BKM can produce excellent results with relatively a small number of nodes for various linear and nonlinear problems. Kang et al[6] and Chen et al[7,8] also developed a meshfree collocation scheme via the nonsingular general solution to calculate the eigenvalue problems. Their method is in essence very similar to the BKM in the evaluation of the homogeneous solution. The differences lie in that the BKM has a symmetric formulation [9] for the problems having mixed boundary conditions and can also solve the inhomogeneous and nonlinear problems. In the BKM, the RBF of different types can be used to evaluate the particular solution without the requirement of mesh. In general, the fundamental and the general solutions of PDE problems can also be considered the radial basis function.

On the other hand, in recent years the multiple reciprocity BEM (MR-BEM)[10] has attracted much attention in the BEM community. The method uses high-order fundamental solutions to approximate high-order homogeneous solutions and then get the particular solutions. By analogy with the MR-BEM, Chen[11] introduced the meshfree boundary particle method (BPM) which combines the RBF and the multiple reciprocity principle to formulate a simple and truly boundary-only meshfree collocation method. The BPM surpasses the MR-BEM in that the method is much easier to program, inherently meshfree, integration-free, and super-convergent observed in a number of numerical experiments. In particular, compared with the MR-BEM, the computing cost in the BPM has been dramatically reduced thanks to an recursive multiple reciprocity scheme introduced by Chen[11]. By analogy with

Fasshauer's Hermite RBF[12], a symmetric BPM formulation is also developed[11].

The advantages and disadvantages of the MR-BEM relative to the DR-BEM are that it does not use inner nodes at all for general inhomogeneous problems but that its mathematical formulation is more complicated and may require more computing cost in some cases. Both the techniques can produce satisfactory solutions for a wide variety of engineering problems. As the MR-BEM versus the DR-BEM[13], the purpose of this study is to distinguish the basic strategies of the BKM and the BPM. Through testifying these two new methods to some typical 2D and 3D PDE problems, we compare their advantages and disadvantages. The rest of this paper is organized as follows. In sections 2 and 3, we give a brief introduction of the BKM and the BPM, followed by section 4 for numerical results and discussions. Finally, section 5 draws some conclusions based on results reported here.

Boundary knot method

To clearly illustrate our idea, consider the following example without loss of generality

$$\Re\{u\} = f(x), \quad x \in \Omega, \tag{1}$$

$$u(x) = R(x), \quad x \subset S_u, \tag{2a}$$

$$\frac{\partial u(x)}{\partial n} = N(x), \quad x \subset S_T, \tag{2b}$$

where $\Re$ is a differential operator, x means a multi-dimensional independent variable, and n is the unit outward normal. The solution of Eq. (1) can be expressed as

$$u = u_h + u_p, \tag{3}$$

where u_h and u_p are the homogeneous and the particular solutions, respectively. The latter satisfies

$$\Re\{u_p\} = f(x), \tag{4}$$

but does not necessarily satisfy boundary conditions. To evaluate the particular solution, the inhomogeneous term is approximated first by

$$f(x) \cong \sum_{j=1}^{N+L} \lambda_j \varphi(r_j), \tag{5}$$

where λ_j are the unknown coefficients. N and $L$are respectively the numbers of knots on the domain and the boundary. The use of interior points is usually necessary to guarantee the accuracy and convergence of the BKM solution. $r_j = \|x - x_j\|$ represents the Euclidean distance norm, and φ is the radial basis function. By forcing approximation representation (5) to exactly satisfy Eq. (4) at all nodes, we can uniquely determine

$$\lambda = A_\varphi^{-1}\{f(x_i)\}, \tag{6}$$

where A_φ is the nonsingular RBF interpolation matrix. Finally, we can get the particular solutions at any point by summing localized approximate particular solutions

$$u_p = \sum_{j=1}^{N+L} \lambda_j \phi \left(\left\| x - x_j \right\| \right), \tag{7}$$

where the RBF ϕ is related to the RBF φ through operator $\Re$. Substituting Eq. (6) into Eq. (7) yields

$$u_p = \Phi A_\varphi^{-1} \left\{ f(x_i) \right\}, \tag{8}$$

where Φ is a known matrix comprised of $\phi\ (r_{ij})$.

On the other hand, the homogeneous solution u_h has to satisfy both the governing equation and the boundary conditions. Unlike the dual reciprocity BEM[1] and MFS[3] using the singular fundamental solution, the BKM[4,5] approximates u_h by means of the corresponding nonsingular general solution, namely,

$$u_h(x) = \sum_{k=1}^{L} \alpha_k u^{\#}(r_k), \tag{9}$$

where k is the index of source points on boundary; $u^{\#}$ is the nonsingular general solution of operator $\Re$. α_k are the desired coefficients. Collocating Eqs. (1) and (2a,b) at all boundary and interior knots in terms of representation (8) and (9), we have the unsymmetric BKM schemes. For the sake of brevity, the details are omitted here[4,5]. In order to get a symmetric BKM scheme for self-adjoint operators, we modify the BKM approximate expression (9) to the homogeneous solution u_h as[9]

$$u_h(x) = \sum_{s=1}^{L_d} a_s u^{\#}(r_s) - \sum_{s=L_d+1}^{L_d+L_N} a_s \frac{\partial u^{\#}(r_s)}{\partial n}, \tag{10}$$

where n is the unit outward normal as in boundary condition (2b), and L_d and L_N are respectively the numbers of knots at the Dirichlet and the Neumann boundary surfaces. The minus sign associated with the second term is due to the fact that the Neumann condition of the first order derivative is not self-adjoint. In terms of expression (10), the collocation analogue equations (1a) and (2a,b) are written as

$$\sum_{s=1}^{L_d} a_s u^{\#}(r_{is}) - \sum_{s=L_d+1}^{L_d+L_N} a_s \frac{\partial u^{\#}(r_{is})}{\partial n} = R(x_i) - u_p(x_i), \tag{11}$$

$$\sum_{s=1}^{L_d} a_s \frac{\partial u^{\#}(r_{js})}{\partial n} - \sum_{s=L_d+1}^{L_d+L_N} a_s \frac{\partial^2 u^{\#}(r_{js})}{\partial n^2} = N(x_j) - \frac{\partial u_p(x_j)}{\partial n}, \tag{12}$$

$$\sum_{s=1}^{L_d} a_s u^{\#}(r_{ls}) - \sum_{s=L_d+1}^{L_d+L_N} a_s \frac{\partial u^{\#}(r_{ls})}{\partial n} = u_l - u_p(x_l). \tag{13}$$

The system matrix of the above equations is symmetric if operator $\Re\{\}$ is self-adjoint. Note that i, s and j are reciprocal indices of the Dirichlet (S_u) and the Neumann boundary (S_Γ) nodes.l indicates response knots inside domain Ω. After the solution of the above simultaneous algebraic equations, we can employ the obtained expansion coefficients α and inner knot solutions u_l to calculate the BKM solution at any knots. It is stressed here that the MFS could not produce the symmetric interpolation matrix at all.

The present form of the BKM uses the expansion coefficient rather than the direct physical variable in the approximation of the boundary value. Therefore, this fashion of the BKM is called as the indirect BKM.

Boundary particle methods

Just like the DR-BEM, the interior nodes are usually necessary in the BKM for inhomogeneous problems. A recent rival with the DR-BEM is the MR-BEM[8], which applies the multiple reciprocity principle to circumvent the domain integral without using any inner node in general. In this section, we will develop a boundary-only RBF scheme called the boundary particle method [11] with the multiple reciprocity principle.

The multiple reciprocity method assumes that the particular solution in Eq. (3) can be approximated by a sum of the higher-order homogeneous solutions, namely,

$$u = u_h^0 + u_p^0 = u_h^0 + \sum_{m=1}^{\infty} u_h^m, \tag{14}$$

where superscript m is the order index of the homogeneous solution. u_h^0 and u_p^0 are equivalent to the homogeneous solution u_h and the particular solution u_p in Eq. (3). Through an incremental differentiation operation via operator $\Re\{\}$, we have successively higher order differential equations:

$$\begin{cases} u_h^0(x_i) = R(x_i) - u_p^0(x_i) \\ \dfrac{\partial u_h^0(x_j)}{\partial n} = N(x_j) - \dfrac{\partial u_p^0(x_j)}{\partial n} \end{cases}, \tag{15a}$$

$$\begin{cases} \Re^0\left\{u_h^1(x_i)\right\} = f(x_i) - \Re^0\left\{u_p^1(x_i)\right\} \\ \dfrac{\partial \Re^0\left\{u_h^1(x_j)\right\}}{\partial n} = \dfrac{\partial\left(f(x_j) - \Re^0\left\{u_p^1(x_j)\right\}\right)}{\partial n} \end{cases}, \tag{15b}$$

$$\begin{cases} \Re^{n-1}\left\{u_h^n(x_i)\right\} = \Re^{n-2}\left\{f(x_i)\right\} - \Re^{n-1}\left\{u_p^n(x_i)\right\} \\ \dfrac{\partial \Re^{n-1}\left\{u_h^n(x_j)\right\}}{\partial n} = \dfrac{\partial\left(\Re^{n-2}\left\{f(x_j)\right\} - \Re^{n-1}\left\{u_p^n(x_j)\right\}\right)}{\partial n} \end{cases}, \quad n = 2, 3, \ldots \tag{15c}$$

where $\Re^n\{\}$ denotes the n-th order operator $\Re\{\}$, say $\Re^1\{\}=\Re\Re^0\{\}$, and $\Re^0\{\}=\Re\{\}$, i and j are respectively the Dirichlet and the Neumann boundary knots. u_p^n is the n-th order of the particular solution defined as

$$u_p^n = \sum_{m=n+1}^{\infty} u_h^m. \tag{16}$$

The m-order homogeneous solution is approximated by

$$u_h^m(x) = \sum_{k=1}^{L} \beta_k^m u_m^{\#}(r_k), \tag{17}$$

where L is the number of boundary nodes, and $u_m^{\#}$ the corresponding m-th order general solutions. Collocating boundary equations (15a,b,c) only on boundary nodes, we have the boundary discretization equations

$$\left.\begin{array}{l} \sum\limits_{k=1}^{L} \beta_k^0 u^0(r_{ik}) = R(x_i) - u_p^0(x_i) \\ \sum\limits_{k=1}^{L} \beta_k^0 \frac{\partial u^0(r_{jk})}{\partial n} = N(x_j) - \frac{\partial u_p^0(x_j)}{\partial n} \end{array}\right\} = b^0, \tag{18a}$$

$$\left.\begin{array}{l} \sum\limits_{k=1}^{L} \beta_k^1 \Re^0\left\{u_1^{\#}(r_{ik})\right\} = f(x_i) - \Re^0\left\{u_p^1(x_i)\right\} \\ \sum\limits_{k=1}^{L} \beta_k^1 \frac{\partial \Re^0\left\{u_1^{\#}(r_{jk})\right\}}{\partial n} = \frac{\partial\left(f(x_j) - \Re^0\left\{u_p^1(x_j)\right\}\right)}{\partial n} \end{array}\right\} = b^1, \tag{18b}$$

$$\left.\begin{array}{l} \sum\limits_{k=1}^{L} \beta_k^n \Re^{n-1}\left\{u_n^{\#}(r_{ik})\right\} = \Re^{n-2}\left\{f(x_i)\right\} - \Re^{n-1}\left\{u_p^n(x_i)\right\} \\ \sum\limits_{k=1}^{L} \beta_k^n \frac{\partial \Re^{n-1}\left\{u_n^{\#}(r_{ik})\right\}}{\partial n} = \frac{\partial\left(\Re^{n-2}\left\{f(x_j)\right\} - \Re^{n-1}\left\{u_p^n(x_j)\right\}\right)}{\partial n} \end{array}\right\} = b^n, \quad n = 2,3,\ldots \tag{18c}$$

In terms of the MR-BEM, the successive process is truncated at some order M, namely, let

$$\Re^{M-1}\left\{u_p^M\right\} = 0. \tag{19}$$

The practical solution procedure is a reversal recursive process:

$$\beta_k^M \to \beta_k^{M-1} \to \cdots \to \beta_k^0. \tag{20}$$

It is noted that due to

$$\Re^{n-1}\left\{u_h^n(r_k)\right\} = u_h^0(r_k), \tag{21}$$

the coefficient matrices of all successive equations are the same, i.e.,

$$Q\beta_k^n = b^n, \quad n = M, M-1, \ldots, 1, 0, \tag{22}$$

Thus, the LU decomposition algorithm is suitable for this task. Finally, the resulting solution is given by

$$u(x_i) = \sum_{n=0}^{M} \sum_{k=1}^{L} \beta_k^n u_n^{\#}(r_{ik}). \tag{23}$$

The BPM differs from the BKM in how to evaluate the particular solution. The former applies the dual reciprocity method, while the latter employs the multiple reciprocity method. The advantage of the BPM over the BKM is that it dose not require interior nodes which may be especially attractive in such problems as moving boundary, inverse problems, and exterior problems. It is expected that like the MR-BEM[8], the truncated order M in the BPM may not be large (usually two or three orders) in a variety of practical uses. The above form of the BPM is unsymmetric. It is rather straightforward to derive the symmetric BPM schemeby replacing Eq. (17) with a representation similar to Eq. (10) and thus, matrix Q in Eq. (22) will be symmetric if operator $\Re\{\}$ is self-adjoint[11].

Numerical experiments and discussions

Figs. 1 and 2 display the 2D and 3D irregular geometries to be tested, which respectively include a triangle cut-out and a two-ball (radii=1, center distance=$\sqrt{2}$) cavity. Unless specified Neumann boundary conditions shown in Fig. 1 and on x=0 surface in Fig. 2, the otherwise boundary are all Dirichlet type. The BKM employs 9 inner nodes for all 2D inhomogeneous case as shown by small crosses in Fig. 1. We applied equally spaced knots on the boundary except on the two-ball surface where the random knots were employed. The Helmholtz and the steady diffusion-reaction equations

$$\nabla^2 u + \gamma^2 u = f(x), \tag{24a}$$

$$\nabla^2 u - \tau^2 u = q(x), \tag{24b}$$

and the steady convection-diffusion equation

$$D\nabla^2 u(x) - v \bullet \nabla u(x) - \kappa u(x) = g(x), \tag{25}$$

are examined, where v denotes a velocity vector, τ is the Thiele parameter, D the diffusivity coefficient, κ represents the reaction coefficient. For the 2D tested examples in this study, the accurate solutions are

$$u = x^2 \sin x \cos y \tag{26}$$

for a 2D inhomogeneous Helmholtz problem ($\gamma = \sqrt{2}$), and

$$u = x^2 e^{-2(x+y)} \tag{27}$$

for a 2D inhomogeneous steady convection-diffusion problems (D=1, $v_x = v_y = v_z$=-2, κ=0,). For 3D tested cases, the accurate solutions are

$$u = \sin x \cos y \cos z \tag{28a}$$

$$\text{and } u = e^{-\sigma x} + e^{-\sigma y} + e^{-\sigma z} \tag{28b}$$

respectively for the 3D homogeneous Helmholtz ($\gamma = \sqrt{3}$) and the convection-diffusion (D=1, $v_x = v_y = v_z$=-σ, κ=0, Peclet number is 24 for σ=1 and 480 for σ=20) problems. The corresponding inhomogeneous function $f(x)$, $q(x)$, $g(x)$ and boundary conditions can easily be derived accordingly. The above problems have been tested in refs. [4,11]. In this study, both the BKM and BPM are used to solve these problems to compare merits and demerits of either method. For the convection-diffusion problems, the Peclet number Pe is defined as

$$Pe = \frac{\left|\vec{v}\right| l}{D}, \tag{29}$$

where l is the characteristic length. For the aforementioned examples, the Peclet number is 16 for the 2D convection-diffusion problem, 24 for σ =1 and 480 for σ=20 in the 3D cases.

The high-order general solutions of Helmholtz, diffusion, and convection-diffusion problems are respectively given by

$$u_m^{\#}(r) = A_m (\gamma r)^{-n/2+1+m} J_{n/2-1+m}(\gamma r), \tag{30}$$

$$u_m^{\#}(r) = A_m (\tau r)^{-n/2+1+m} I_{n/2-1+m}(\tau r), \tag{31}$$

$$u_m^{\#}(r) = A_m (\mu r)^{-n/2+1+m} e^{\frac{v \cdot r}{2D}} I_{n/2-1+m}(\mu r), \quad n \geq 2, \tag{32}$$

where n is the dimension of the problem; m denotes the order of the general solution; J and I respectively represent the Bessel and the modified Bessel functions of the first kind; $A_m = A_{m-1}/(2 * m * \gamma^2)$, A_0=1;

$$\mu = \left[\left(|v|/2D \right)^2 + \kappa / D \right]^{\frac{1}{2}}. \tag{33}$$

For the 2D and 3D cases, the Bessel functions in formulas (30-32) can be restated by sine and exponential functions in an explicit way[4,11]. In this study, the second-order high order general solutions are used as the radial basis function in the BKM approximation of the particular solution. The L_2 norms of relative errors are calculated by the numerical solutions at 364 nodes for 2D and 500 nodes for 3D. The absolute error is taken as the relative error if the absolute value of the accurate

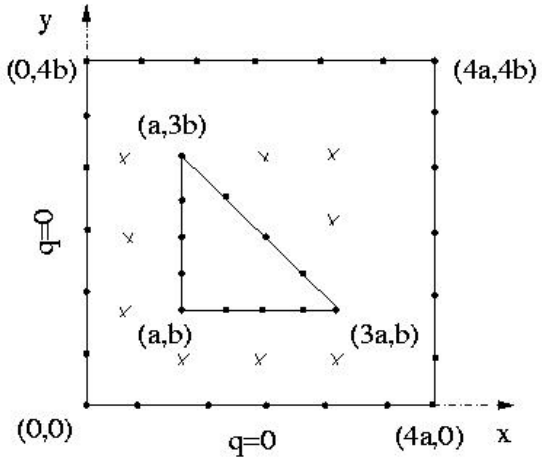

Fig. 1. Configuration of a square with a trigeometric cutout

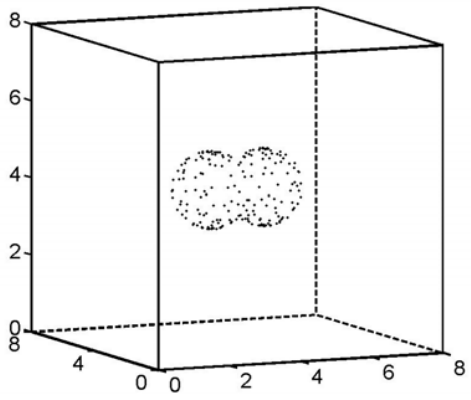

Fig. 2. A cube with a two-ball cavity

solution is less than 0.001. Note that different numbers and locations of inner and boundary nodes are used for BKM and BPM coefficients and for L_2 norm of relative errors.

Numbers inside parentheses in all tables below indicate the numbers of the boundary plus the inner nodes used by the respective method. The experimental results of the 2D Helmholtz problem are displayed in Table 1. It is found that both methods produce very accurate solutions with a small number of nodes. Like the DR-BEM, the BKM is found somewhat sensitive to the location and the number of inner nodes, while the BPM does not need any inner nodes at all.

Table 1: L_2 norm of relative errors for the 2D inhomogeneous Helmholtz problem by the BKM and the BPM

BKM	1.9e-3 (26+9)	9.3e-5 (33+9)
BPM	2.8e-3 (26)	6.8e-4 (33)

The BKM and BPM results for the 2D steady convection-diffusion problem are listed in Table 2. It is noted that the peak solution accuracy of the BKM and the BPM is around 0.0001. It is observed that the BKM seems to perform more stable than the BPM in this case despite more computing effort.

Table 2: L_2 norm of relative errors for the 2D inhomogeneous steady convection-diffusion problem by the BKM and the BPM

BKM	1.9e-3 (19+9)	2.4e-4 (26+9)	2.37e-4 (33+9)
BPM	1.6e-3 (19)	2.4e-4 (26)	3.9e-3 (33)

Table 3 illustrates the numerical results for the 3D problems by the BKM. Relative to the previous 2D case, the 3D case requires more nodes due to not only one more dimension but also larger computational domain and more complicated boundary surface. It is noted that the solution accuracy for a higher Peclet number tends to be better. On the other hand, despite the fact that the present BPM scheme produces very accurate solution of the 2D problems, the method can not get the correct solution of the 3D problems. The cause of this failure is still under investigation.

Table 3: L_2 norm of relative errors for 3D homogeneous Helmholtz and convection-diffusion problems by the BKM.

Helmholtz	4.6e-3 (298)	1.7e-4 (466)
Convection-diffusion (Pe=24)	9.0e-3 (136)	2.2e-3 (298)
Convection-diffusion (Pe=480)	8.8e-15 (136)	6.8e-15 (178)

Conclusions

The BKM and the BPM circumvent the troublesome singular integral inherent in the BEM and are very easy to learn and program. For the same applications, both methods produce the solutions of similar accuracy. In addition, both techniques are essentially meshfree, spectral convergence and symmetric. It is noted that unlike the MR-BEM, the BPM does not need to generate more than one interpolation matrix via the recursive multiple reciprocity technique, which significantly reduces the computing effort and storage requirements. In some cases, the BPM requires less computing effort than the BKM thanks to the recursive multiple reciprocity technique. In addition, the solution accuracy of the BKM also depends largely on the proper choice of the RBF and the number and the location of inner nodes to evaluate the particular solution. As of the stability, the BKM performs better than the BPM in this study. In particular, the BPM has failed to solve the 3D problems

by now.

Similar to the comparisons between the DR-BEM and MR-BEM[13], the BKM may be mathematically more simple and generally more applicable than the BPM, while the latter has advantage not requiring inner nodes for inhomogeneous problems and is very suitable for problems whose higher-order homogeneous solution quickly tends to zero. In contrast, the BKM appear more flexible in general engineering applications. The major drawbacks of both the BKM and the BPM are severely ill-conditioned and costly full matrix for large discretization equations, which may significantly be eased by some preconditioning techniques such as the fast multipole, panel clustering, and H matrix methods, a subject still under intensive investigation.

References

1. D. Nardini, and C.A. Brebbia, A new approach to free vibration analysis using boundary elements, *Applied Mathematical Modeling* **7**, 157-162, (1983).
2. E.J. Kansa, Multiquadrics: A scattered data approximation scheme with applications to computational fluid-dynamics. *Comput. Math. Appl*. **19**, 147-161, (1990).
3. M.A. Golberg and C.S. Chen, The method of fundamental solutions for potential, Helmholtz and diffusion problems. In *Boundary Integral Methods - Numerical and Mathematical Aspects,* (Ed. by M.A. Golberg), pp. 103-176, Comput. Mech. Publ., (1998).
4. W. Chen and M. Tanaka, A meshless, exponential convergence, integration-free, and boundary-only RBF technique, *Computers and Mathematics with Applications* **43**, 379-391, (2002).
5. Y.C. Hon and W. Chen, Boundary knot method for 2D and 3D Helmholtz and convection-diffusion problems with complicated geometry, *Int. J. Numer. Methd. Engng.* **56**(13), 1931-1948, (2003).
6. S. W. Kang, J. M. Lee, Free vibration analysis of arbitrarily shaped plates with clamped edges using wave-type functions, *J. Sound Vibr*. **242**(1), 9-26, (2001).
7. J. T. Chen, M. H. Chang, K. H. Chen, S. R. Lin, The boundary collocation method with meshless concept for acoustic eigenanalysis of two-dimensional cavities using radial basis function, *J. Sound Vibr*. **257**(4), 667-711, (2002).
8. J. T. Chen, M. H. Chang, K. H. Chen, I. L. Chen, Boundary collocation method for acoustic eigenanalysis of three-dimensional cavities using radial basis function, *Comput. Mech*. **29**, 392-408, (2002).

9. W. Chen, Symmetric boundary knot method, *Engng. Anal. Bound. Elem.* **26**(6), 489-494, (2002).

10. A.J. Nowak and A.C. Neves (ed.). *The Multiple Reciprocity Boundary Element Method*. Comput. Mech. Publ., Southampton, UK, (1994).

11. W. Chen, Meshfree boundary particle method applied to Helmholtz problems, *Engng. Anal. Bound. Elem.* **26,** 577–581, (2002).

12. G.E. Fasshauer. Solving partial differential equations by collocation with radial basis functions. In: Mehaute A, Rabut C, Schumaker L. *Proceedings of Chamonix*; p. 1–8, (1996).

13. A.J. Nowak and P. W. Partridge, Comparison of the dual reciprocity and the multiple reciprocity methods, *Engng. Anal. Bound. Elem.* **10**, 155-160, (1992).